Hot Spot Ignition in White Dwarfs – One-zone Ignition Times

L. Jonathan Dursi
CITA, University of Toronto, Toronto, ON, M5S 3H8, Canada
Frank X. Timmes
Theoretical Astrophysics Group, Los Alamos National Laboratory, Los Alamos, NM, 87545, USA

Type Ia supernovae are almost certainly caused by the incineration of a turbulent carbon-oxygen white dwarf. Local hot spots ignite and either fizzle out, or begin propagating burning as a deflagration or a detonation, in which the carbon and oxygen is consumed. These burning pockets may then rise harmlessly upwards, or may be large enough to cause a large fraction of the dwarf to burn.
Although the basic picture is understood, the details of igniting these hot spots remains fuzzy. In this work, we begin the process of understanding the ignition of these hotspots by examining the burning of one zone of the white dwarf.

1. Introduction

The standard model for supernovae of type Ia involves burning beginning as a subsonic deflagration in a Chandrasekhar-mass white dwarf. Progress has been made in recent years in understanding these events through multidimensional reactive simulations where the initial burning is prescribed as an initial condition of one or more sizable bubbles already burning material at time zero. However, the initial ignition process by which such bubbles begin burning – whether enormous 50 km bubbles [Plewa et al. 2004] or smaller igniting points [Woosley et al. 2004, García-Senz and Bravo 2005] – remains poorly understood. Further, if there is later in evolution a transition to a detonation [Gamezo et al. 2004], this ignition process, too, must be explained. Here we begin examining the ignition process by considering the simplest ignition possible – that of a single zone.

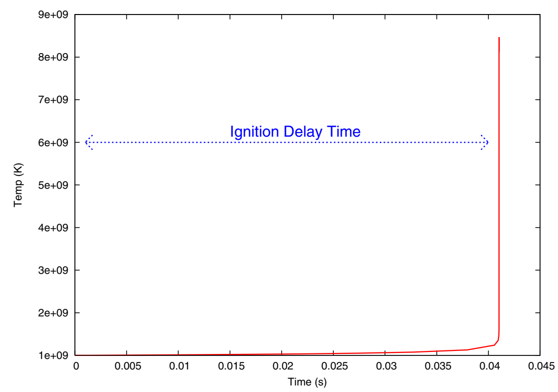

Figure 1: Temperature evolution for burning constant-pressure zone with $X_{C12} = 1.0$, $T_o = 10^9$K, $\rho_o = 5 \times 10^8$g cm^{-3}. Because of the strong temperature dependence, most of the burning happens 'all at once'.

2. Ignition Times

Astrophysical combustion, like most combustion, is highly temperature-dependent (for example, Williams [1985], Glassman [1996].) Rates for the exothermic reactions which define the burning process are generally exponential or near-exponential in temperature (eg, Caughlan and Fowler [1988]). Thus a hotspot can sit 'simmering' for a very long time, initially only slowly consuming fuel and increasing its temperature as an exponential runaway occurs. If fuel depletion were ignored, and ignoring hydrodynamical effects, the temperature of the spot would become infinite after a finite period of time. This time is called the ignition time, or ignition delay, or sometimes induction time, τ_i. After ignition starts, burning proceeds for some length of time τ_b.

For burning problems of interest, of course, fuel depletion is important, and no quantities become infinite; however, the idea of an ignition delay time still holds (see Fig. 1). If the energy release rate for most of the evolution of the burning is too small to have significant hydrodynamical effects, and if the timescale over which burning 'suddenly turns on' is much shorter than any other hydrodynamical or conductive timescales, then the burning of such a hotspot can be treated, as an excellent approximation, as a step function where all energy is released from $t = \tau_i$ to $t = \tau_i + \tau_b$. In many problems, where $\tau_b \ll \tau_i$, this can be further simplified to burning occurring only at $t = \tau_i$. Where such an approximation (often called 'high activation-energy asymptotics') holds, it greatly simplifies many problems of burning or ignition, reducing the region of burning in a flame to an infinitesimally thin 'flamelet' [Matalon and Matkowsky 1982] surface, for instance, or the structure of a detonation to a 'square wave' [Erpenbeck 1963]. Where this approximation does not hold – such as if slow β-decay processes are energetically important – the simplification of burning happening only over $\tau_i \le t \le \tau_i + \tau_b$ often remains a useful simplification.

If the burning is happening in an ideal gas, or in a material with some other simple equation of state (where, for instance, the specific heat is constant in temperature), it is fairly easy to write down approximate ignition times for various burning laws. In a white dwarf, however, where the material is partially degenerate or relativistic and the equation of state is quite complicated [Timmes and Swesty 2000], no such closed-form expression can be written. In this poster, we numerically integrate burning and temperature evolution of a zone of white dwarf material, and measure the ignition times as a function of the initial temperature, density, composition, and whether the evolution was assumed to be constant-density or constant-pressure. The results are simple, moderately accurate, fitting formula, and some direction for future applications are discussed.

3. Calculations

We performed a series of calculations of 1-zone burning of carbon/oxygen mixtures for the purposes of measuring ignition times of carbon-oxygen mixtures under these conditions. Time evolutions were generated as in Fig. 1.

For each of two burning conditions – burning at constant volume and constant pressure – over 2500 initial conditions were examined, in a grid of initial densities, temperatures, and initial carbon fraction. In the conditions chosen here, densities and temperatures were selected to be relevant to the inner regions of a near-Chandrasekhar-mass white dwarf. For burning, a 13-isotope α chain was used [Timmes 1999], and a Helmholtz free energy based stellar equation of state [Timmes and Swesty 2000] maintained the thermodynamic state.

To cover the wide range of burning times within each simulation, the timestep was increased or decreased depending on rate of change of fuel abundance. The timestep was varied by up to a factor of two in each step, to try to keep the change of fuel within the range $10^{-5} - 10^{-7}$ per timestep. The final ignition time, when the simulation was stopped, was defined to be time when 90% of the carbon was consumed, although the time reported was found to be insensitive to endpoint chosen.

Over the initial conditions chosen, ignition times varied from 10^{-13} s to 10^{+8} s.

Constant-Pressure fitting formula:

$$\tau_{i\mathrm{CV}}(\rho, T, X_{C12}) = 2.16 \times 10^{-13}\mathrm{sec} \times \exp(16.0\hat{T}_9^{-1}(1 + 10.3\hat{T}_9^{-1})) \times\hat{\rho}_8^{-2}(1 + 2.91\hat{\rho}_8^{-1})$$

where

$$\hat{T}_9 = \frac{T}{10^9\mathrm{K}} + 1.68$$

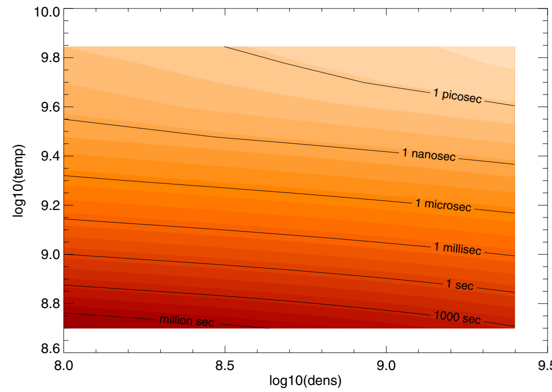

Figure 2: Contour plot of ignition time as a function of initial density and temperature for a constant-pressure ignition of pure carbon.

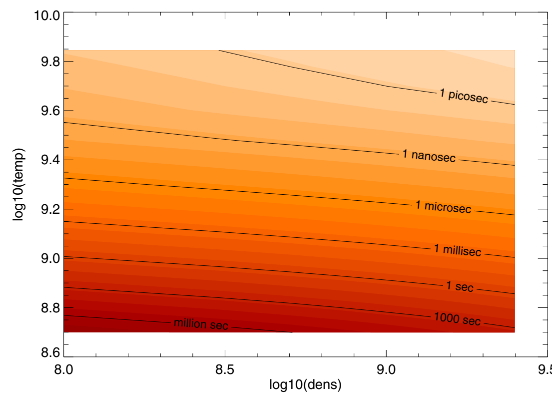

Figure 3: Contour plot of ignition time as a function of initial density and temperature for a constant-volume ignition of pure carbon. Differences between constant-pressure and constant-volume ignition times under these moderately degenerate conditions are on order a factor of two.

$$\hat{\rho}_8 = \frac{\rho X_{C12}}{10^8\mathrm{g\,cm}^{-3}} + 0.865$$

Constant-Volume fitting formula:

$$\tau_{i\mathrm{CV}}(\rho, T, X_{C12}) = 2.80 \times 10^{-13}\mathrm{sec} \times \exp(15.2\hat{T}_9^{-1}(1 + 11.4\hat{T}_9^{-1})) \times\hat{\rho}_8^{-2}(1 + 1.85\hat{\rho}_8^{-1})$$

where

$$\hat{T}_9 = \frac{T}{10^9\mathrm{K}} + 1.72$$

$$\hat{\rho}_8 = \frac{\rho X_{C12}}{10^8\mathrm{g\,cm}^{-3}} + 0.837$$

The fits are good to $\approx 50\%$ between 10^{-9} sec and 1 sec for temperature and density range as shown, and X_{C12} from 0.5 to 1.0, as shown for instance in Fig. 4;

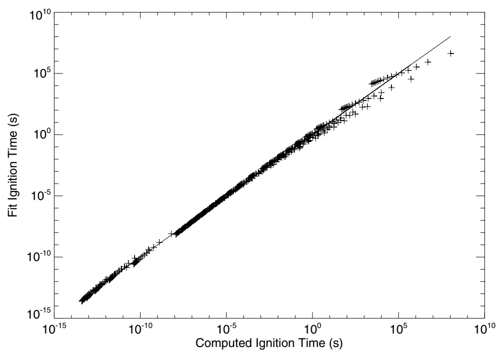

Figure 4: Fit results vs. calculated results for constant-volume pure carbon ignition.

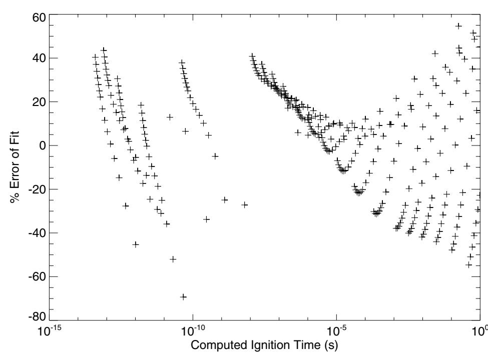

Figure 5: Fit residuals vs. calculated results for constant-volume pure carbon ignition.

however, as the residuals indicate in Fig. 5, the results are not likely to be meaningful outside of the range of conditions calculated here.

4. Detonation structure

A detonation can be thought to consist of three states; the state the detonation propagates into; the post-shock state; and the completely burned state. For a steady-state Chapman-Jouget (CJ) detonation, these states can be computed for a given unshocked medium (see for instance Glassman [1996].) Since we now can compute ignition times for the intermediate state, we can estimate the width of the CJ detonation, l_{CJ}, as equal to the ignition time at the intermediate state multiplied by the material velocity in that state.

In the case of a detonation into a very low-density, cold material, the material immediately behind the shock will still not burn significantly for a length of time equal to the ignition time, and we will have a square wave detonation. For conditions relevant to near the core of a white dwarf, however, the intermediate state of a shock will typically have temperatures on order 5×10^9 K – that is, temperatures which are near the maximum temperature which will be obtained by burning. Even in these cases, this estimate of l_{CJ} provides a good measure of the thickness of the detonation structure behind the shock, as is shown in Fig 6 and Fig 7.

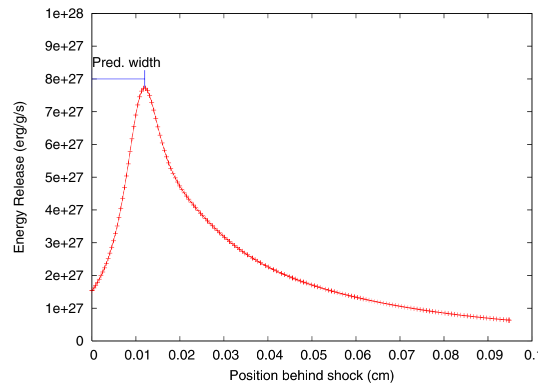

Figure 6: Energy release rate from nuclear reactions behind the shock of a leftward-traveling ZND detonation into a pure-carbon quiescent medium of $\rho_o = 10^8\,\mathrm{g\,cm^{-3}}$, $T_o = 5 \times 10^7$K. The shocked state is $\rho_s = 2.97 \times 10^8\,\mathrm{g\,cm^{-3}}$, $T_s = 4.2 \times 10^9$K, and the incoming fuel velocity is $4.0 \times 10^8\,\mathrm{cm\,s^{-1}}$. For the shocked material, the predicted ignition time is 3×10^{-11}s. Even in this case, where the shocked temperature is so high that significant burning occurs immediately, and the 'square wave' detonation structure does not apply, the predicted $l_{CJ} = 1.2 \times 10^{-2}$cm correctly matches the peak of the reaction zone.

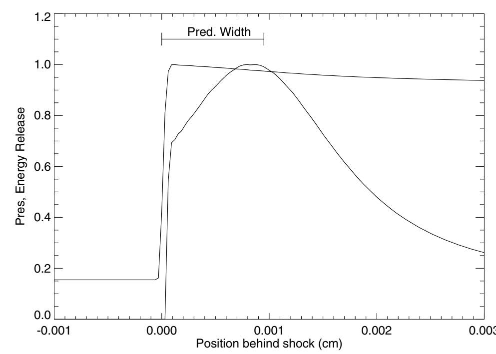

Figure 7: Pressure and energy release rate, plotted relative to their maximum values, behind a leftward-traveling slightly overdriven detonation into the same material as in the previous figure, calculated by a hydrodynamics code. The line above the plotted quantities shows the predicted l_{CJ} calculated with the observed values in the intermediate state.

5. Ignition of a Spherical Detonation

Emergence of a detonation in a homogeneous, exothermically reacting medium can occur in two steps. The first step processes the medium to create conditions ripe for the onset of detonation. The events leading up to preconditioning may vary from one scenario to the next, but typically, at the end of this stage the medium is hot and in a state of non-uniformity (e.g., turbulent motions). The second step forms the detonation wave via interactions between exothermic processes and hydrodynamics.

Consider the case when the preconditioned medium has an initial linear gradient of temperature. For shallow gradients, the result is a decelerating supersonic reaction wave, a weak detonation, whose trajectory is dictated by the initial temperature profile, with only weak intervention from hydrodynamics. If the domain is long enough, or the gradient less shallow, the wave slows down to the CJ speed and undergoes a swift transition to the ZND structure.

For sharp gradients, the path to detonation is through an accelerating pulse that runs ahead of the reaction wave. This rearranges the ignition-time distribution to one that has little resemblance to the ignition-time distribution of the initial temperature gradient. The pulse amplifies and steepens, transforming itself into a lead shock, an induction zone, and a following fast deflagration. If the domain is long enough, these three entities gradually transform to the ZND structure.

In this study we consider a step function initiation profile; the limiting case of a infinite initial temperature gradient. A Sedov explosion is generated by depositing an energy into a well defined mass region; and the evolution of the structure described above ensues.

Naively, the condition for a successful detonation ignition would be that $R_{CJ} \approx l_{CJ}$, since a detonation structure of width l_{CJ} must be set up before the shock speed becomes too slow. However, experimentally this is known to be far too lenient a condition, and R_{CJ} must be orders of magnitude larger than l_{CJ}.

This has been explained by, for instance, He and Clavin [1994]. Curvature has a significant nonlinear effect on the structure of a detonation; looking at a pseudo-steady calculation of a detonation with curvature, they find that for a near-CJ steady detonation to exist and be stable requires curvature to be extremely small. The condition found by the authors requires $R_{CJ} \approx 300 l_{CJ}$.

Given our calculations for l_{CJ}, we can test the applicability of this result to detonations in degenerate white dwarf material. The reason that the He & Clavin's result may give reasonable guidance, despite being derived for terrestrial reacting flows but used here for nuclear burning under degenerate/relativistic conditions, is that it's a calculation of non-linear curvature effects on detonation structure, which ultimately comes down to a ratio of length scales. He & Clavin use the ideal gas EOS assumption to calculate the detonation length scale from first principles and compare it to the curvature length scale. The EOS

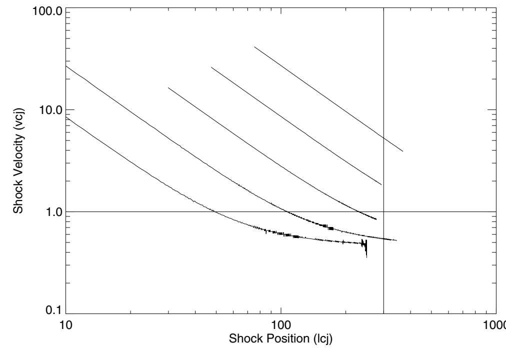

Figure 8: Shock velocity vs. shock position for a Sedov explosion, without burning, into pure carbon medium of $\rho_o = 10^8 \,\mathrm{g\,cm^{-3}}$, $T_o = 5 \times 10^7$K. Shock velocity is given in units of the CJ detonation speed, ($D_{CJ} \approx 1.2 \times 10^9 \,\mathrm{cm\,s^{-1}}$) and shock position in units of CJ detonation width ($l_{CJ} \approx 0.012$cm). Input energies are, top to bottom, 10^{30},10^{29},10^{28}, 10^{27}, and 10^{26} ergs within a radius of 0.0015 cm.

only comes in through the detonation length scale, and doesn't matter much afterwards.

In Fig. 8, we see the shock speed of a Sedov explosion for various input energies. By the criterion of He and Clavin, with this configuration we would expect a successful ignition of a detonation with an input energy of 10^{29} ergs and greater, and an unsuccessful ignition with an input energy of 10^{28} ergs and less. (It is also interesting to note that the early stages of evolution of the shocks which would later successfully ignite a detonation are relativistic.)

To test this prediction, we can run the same calculations with burning. The results are shown in Fig. 9. We see that neither the 10^{28} nor the 10^{29} erg Sedov explosions result in sustained detonations, which would asymptote to a velocity equal to the CJ detonation velocity. This may be due the EOS of the degenerate material playing a more significant role than is obvious in the He & Clavin work, or it may be a result of the fact that the location of peak nuclear energy release underestimates the required structure of the detonation, as significant amounts of energy continue to be released well behind the peak of the burning, as shown in Fig 6 and Fig 7. Further examination of the failure of this criterion will be left to future work.

6. Conclusion

We have presented ignition times for carbon-oxygen mixtures at densities and temperatures relevant to the cores of near-Chandrasekhar-mass white dwarfs. Even in cases where high-energy asymptotics does not hold, such as in detonations in these degenerate materials,

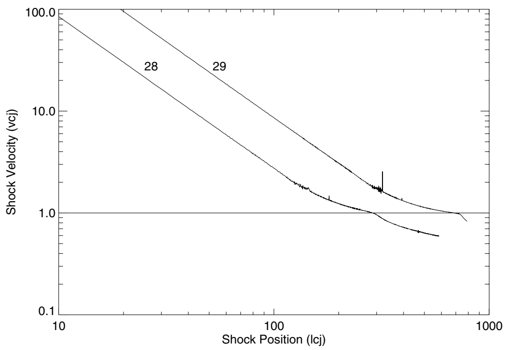

Figure 9: Shock velocity vs. shock position for a Sedov explosion, with burning. Conditions and scales are as in the previous figure. Note that when the shock velocity approaches the CJ detonation velocity from above, burning begins to effect the shock speed, but fails to sustain a CJ detonation for the case of input energies of 10^{28} and 10^{29} ergs.

the ignition time is physically meaningful, giving estimates of detonation thickness that compare well with ZND and hydrodynamical calculations. However, the square wave approximation is a poor match to detonations in such degenerate conditions, and caution must be taken in applying square-wave detonation results from chemical combustion to astrophysical thermonuclear detonations.

References

T. Plewa, A. C. Calder, and D. Q. Lamb, ApJL **612**, L37 (2004).

S. E. Woosley, S. Wunsch, and M. Kuhlen, ApJ **607**, 921 (2004).

D. García-Senz and E. Bravo, A&Ap **430**, 585 (2005).

V. N. Gamezo, A. M. Khokhlov, and E. S. Oran, Physical Review Letters **92**, 211102 (2004).

F. A. Williams, *Combustion Theory* (Benjamin/Cummings Publishing Company, Menlo Park, California, 1985), 2nd ed.

I. Glassman, *Combustion* (Academic Press, San Diego, 1996), 3rd ed.

G. R. Caughlan and W. A. Fowler, Atomic Data and Nuclear Data Tables **40**, 283 (1988).

M. Matalon and B. J. Matkowsky, J. Fluid Mech. **124**, 239 (1982).

J. J. Erpenbeck, in *9th International Symposium on Combustion* (Academic Press, New York, 1963), pp. 442–453.

F. X. Timmes and F. D. Swesty, ApJSS **126**, 501 (2000).

F. X. Timmes, ApJSS **124**, 241 (1999).

L. He and P. Clavin, J. Fluid Mech. **277**, 227 (1994).